Electronic and vibronic cluster models for the $^4T_2(G)$ level of d^5 ions in tetrahedral symmetry

R. Parrot
Institut Universitaire de Formation des Maîtres et Institut d'Etudes Supérieures de Guyane, Boîte Postale 792, 97337 Cayenne Cedex, France

D. Boulanger
Laboratoire d'informatique, Maîtrise de Sciences Physiques, Bâtiment 479, Université de Paris Sud, 91405 Orsay Cedex, France
(Received 22 December 2004; revised manuscript received 23 February 2006; published 8 August 2006)

Electronic and vibronic cluster models are proposed to elaborate a general model for the $^4T_2(G)$ orbital triplet levels of d^5 ions in tetrahedral symmetry. These models involve perturbation schemes and the diagonalization of the molecular electronic structure and vibronic Hamiltonian. First, the electronic fine structure is determined from the first- and second-order molecular spin-orbit (MSO) interaction. Then, Ham's perturbation model for vibronic interactions is used in conjunction with the molecular model to analyze the vibronic interactions corresponding to a strong coupling to ε-vibrational modes. Then, a more general model is considered to account for the energy-level schemes and the strong intensity transfer observed, for example, on the fine structure lines of the $^4T_2(G)$ level of Mn^{2+} in ZnS and ZnSe. This model involves the diagonalization of the vibronic Hamiltonian for the $^4T_2(G)$ level and a perturbation model to account for vibronic interactions with all other multiplets of the d^5 configuration. It is shown that the energy-level schemes as well as the strong intensity transfer of the fine structure lines of the $^4T_2(G)$ level of Mn^{2+} in ZnS and ZnSe are very well accounted for from the electronic molecular model involving the first- and second-order MSO interaction and from the proposed diagonalization and perturbation models for the coupling to ε-vibrational modes.

DOI: 10.1103/PhysRevB.74.064302 PACS number(s): 71.55.Eq, 71.55.Gs, 71.70.Ch, 71.70.Ej

I. INTRODUCTION

The fluorescent and excited electronic and vibronic levels of d^5 ions in crystals[1–12] and nanoclusters (Refs. 13–16) (NC) have long been studied experimentally and theoretically. Concerning the excited states of Mn^{2+} and Fe^{3+} in II–VI and III–V crystals, several studies have been devoted to the determination of the lifetimes of the $^4T_1$ fluorescent level and to the analysis of the fine structure lines of the $^4T_1$ fluorescent level and excited levels at higher energy such as the $^4T_2(G)$ and $^4E(G)$ levels. For example, detailed analyses of the electronic and vibronic structures of the $^4T_1(G)$ fluorescent level of Mn^{2+} in ZnS, ZnSe,[1,2] and in GaP (Ref. 3) have been performed. The $^4T_2(G)$ level of Mn^{2+} has been studied in ZnS and ZnSe.[4–6] For Fe^{3+}, the optical levels have been studied in ZnS,[7] ZnO,[8] GaAs,[9] GaN,[10,11] and InP.[12]

For NCs, great attention has been paid to the fluorescent bands observed in undoped and manganese-doped ZnS NCs (Refs. 13 and 14) and ZnSe NCs.[15] From lifetimes measurements, it has been shown that the intense emission band observed in ZnS: Mn^{2+} NCs, in the range of the emission observed in crystals, is due to traps which show very short lifetimes and Mn^{2+} centers with a lifetime similar to that observed in crystals.[14] For ZnSe: Mn^{2+} NCs, a broad emission band observed at 2.1 eV has been attributed to Mn^{2+} centers.[15] For ZnS NCs, excitation spectra of Mn^{2+} ions from levels at higher energy as levels $^4T_2(G)$, $^4E(G)$, etc.,…, and also from the absorption band of the fluorescent level $^4T_1(G)$, have been reported and compared with those observed in crystals in order to determine the vibronic interactions and the Huang-Rhys factors S for this level in NC's.[16] ($S=E_{JT}/\hbar\omega$, where E_{JT} is the Jahn-Teller energy and $\hbar\omega$ is the energy of an effective phonon.)

The aim of this paper is to propose an electronic molecular model and vibronic models for the fine structure of the $^4T_2(G)$ level of Mn^{2+} in ZnS and ZnSe. An electronic molecular model analogous to that used to analyze the fluorescent levels in these compounds[1,2] and indications concerning the vibronic models have been briefly presented in Ref. 6.

Concerning the structure of the $^4T_2(G)$ level of Mn^{2+} in ZnS and ZnSe, uniaxial stress experiments,[4] Zeeman experiments,[5] and an analysis of the relative amplitudes of the fine structure lines,[4] that is, of the relative dipole strengths (RDSs), have shown that the vibronic coupling is to ε-vibrational modes only (there is no coupling to τ_2-vibrational modes since no splitting and no broadening of the Γ_8 levels has been observed when applying uniaxial stresses along a [111] axis) and that the level ordering of the observed fine structure lines, for increasing relative energy, is $\Gamma_8(5/2)$ $[W\Gamma_8(5/2)=0]$, Γ_6 $(W\Gamma_6=4\ cm^{-1})$, and $\Gamma_8(3/2)$ $[W\Gamma_8(3/2)=34\ cm^{-1}]$ for ZnS, and $\Gamma_8(5/2)$ $[W\Gamma_8(5/2)=0]$ and Γ_6 $(W\Gamma_6=10\ cm^{-1})$ for ZnSe. The transition from the fundamental $^6A_1$ level to the Γ_7 level is not observed since it is strictly forbidden in tetrahedral symmetry. Furthermore, the experimental RDS of the $^6A_1 \rightarrow \Gamma_8(3/2)$ transition is very weak in ZnS and is not observed in ZnSe.

Concerning the theoretical models, it has long been shown (see Ref. 4) that, at least in the case of Mn^{2+} in ZnS and ZnSe, previous models based on the crystal-field (CF) model for the electronic structure and perturbation models for weak or strong vibronic interactions cannot account for both the observed energies and the strong intensity transfer from the fine structure line at higher energy to vibrational levels. The model proposed in Ref. 4 was obtained by diagonalizing the vibronic interactions for the first-order spin-orbit (SO) interaction of the $^4T_2$ level. The model approximately

accounted for the energy levels and intensity transfers; *however, for ZnSe, it was necessary to invoke a SO interaction much larger than that predicted by the CF model.*

The extended cluster model giving the monoelectronic and multielectronic wave functions for the orbital triplet states, the first- and second-order MSO interaction, as well as Ham's cluster model and perturbation models for the vibronic coupling to ε-vibrational modes, are presented in Sec. II A. The diagonalization of the vibronic Hamiltonian for the $^4T_2(G)$ level and the perturbation model for the contribution of the other multiplets of the d^5 configuration is presented in Sec. II B. The electronic and vibronic structures for level $^4T_2(G)$ of Mn^{2+} in ZnS and ZnSe, as deduced from Ham's perturbation model, are presented in Sec. III. In Sec. IV, the experimental results for levels $^4T_2(G)$ of Mn^{2+} in ZnS and ZnSe are compared with the theoretical results. It is shown that the molecular and vibronic cluster models proposed in Sec. II B account very well for the energy level scheme and for the very strong selective intensity transfer on level $\Gamma_8(3/2)$ for the $^4T_2(G)$ levels of Mn^{2+} in ZnS and ZnSe.

II. MOLECULAR AND VIBRONIC CLUSTER MODELS

A. Molecular electronic model and Ham's perturbation model for the vibronic coupling to ε-vibrational modes

The first- and second-order MSO interactions for the $^4T_2(G)$ level of Mn in ZnS and ZnSe are calculated by adapting the molecular model described in Ref. 1 for level $^4T_1(G)$. For the convenience of the reader, we will briefly recall the molecular model.

The operator H_{SOm} describing the MSO interaction is defined in terms of the spin-orbit interaction for the cation, the total angular momentum Ω^i of electron i of the ligands, and the complex component s_q^i of the spin operators for electron i by[18]

$$H_{SOm} = \sum_q \sum_i \sum_u [\zeta_M(r_{iM})\mathbf{l}_{Mu}^i + \zeta_L(r_{iL})\Omega_u^i]s_q^i,$$

$u=x$ or y if $q=\pm 1$ and $u=z$ if $q=0$. $\mathbf{l}_{iM}$ and $\mathbf{l}_{iL}$ are one-electron orbital operators for the metal and the ligands, respectively. ζ_M and ζ_L are the spin-orbit coupling constants for the electrons of the cation and of the ligands, respectively. It must be noted here that, in molecular models, ζ_M and ζ_L depend on the charge of the cation and of the ligands.[18] The MSO interaction is expressed in terms of the angular momentum τ_u^i of electron i and in terms of the complex component s_q^i of the spin operators for electron i by[18]

$$\tau_u^i = \zeta_M(r_{iM})\mathbf{l}_{Mu}^i + \zeta_L(r_{iL})\Omega_u^i.$$

The MSO interaction will be characterized by the following matrix elements ζet_2 and $\zeta t_2 t_2$ of τ:

$$\zeta et_2 = (i/2)\langle e\varepsilon|\tau_z|t_2\zeta\rangle = a^d b^d \zeta_M + [1/(2\sqrt{3})]b^{\pi p}(a^{\pi p} + a^{\sigma p}\sqrt{2})\zeta_L$$

and

$$\zeta t_2 t_2 = -i\langle t_2\xi|\tau_z|t_2\rangle = (a^d a^d - a^p a^p)\zeta_M + a^{\pi p}(a^{\sigma p}\sqrt{2} - a^{\pi p}/2).$$

In the chosen cluster model, the mixing coefficients a and b are defined from the monoelectronic molecular orbitals $4t_2$ and $2e$ written in terms of the monoelectronic orbitals of the $3d$ and $4p$ electrons of the cation, and in terms of the orbitals σs, σp, and πp of the ligands as

$$|t_2\gamma\rangle = a^d|dt_2\gamma\rangle + a^p|pt_2\gamma\rangle + a^{\sigma s}|\sigma s t_2\gamma\rangle + a^{\sigma p}|\sigma p t_2\gamma\rangle + a^{\pi p}|\pi p t_2\rangle,$$

where $\gamma=\xi$, η, or ζ refers to the components of the molecular monoelectronic level $4t_2$ and

$$|e\gamma\rangle = b^d|de\gamma\rangle + b^{\pi p}|\pi pe\gamma\rangle,$$

where $\gamma'=\theta$ or ε refers to the components of the molecular monoelectronic level $2e$.

The multielectronic wave functions for the multiplets are obtained by diagonalizing the electrostatic matrices of Sugano, Tanabe, and Kamimura for all multiplets of the configuration d^5 by using the cubic field parameter Dq and the Racah parameters B and C.[19] It has long been shown that, in molecular models, the energies of the multiplets are described by exchange and Coulomb integrals, which in cubic symmetry, depend on ten coefficients.[20] Since it is very difficult to determine all relevant coefficients, either theoretically or from fittings of the energy levels, we will simply use Racah parameters B and C as deduced from fitting of the experimental energy levels. In earlier models, tentative fittings of the energy levels were performed by taking $B/C \approx 4.5$ as given by the CF model restricted to Mn^{2+}.[19] However, this constraint has long been abandoned since it is not justified in molecular models and since the fitting of the energy levels is better when this constraint is dropped. In the following, several sets of values for B, C, and Dq will be considered in order to test their influence on the theoretical structure of the studied levels.

A program has been elaborated to calculate all relevant matrix elements of the first- and second-order MSO interaction for the multielectronic wave functions. Finally, the electronic fine structure is calculated in the spinor group T_d^*.[20]

The *electronic* energy levels are described by the following electronic equivalent operator:[17]

$$H_{eq} = c_{T1}\mathbf{lS} + c_E(2/3)(l_\theta S_\theta + l_\varepsilon S_\varepsilon) + c_{A1}(1/3)\mathbf{l}^2\mathbf{S}^2 + c_{T2}(1/2)(l_\xi S_\xi + l_\eta S_\eta + l_\zeta S_\zeta).$$

The index in the c_Γ's means that the operators span the representation Γ of the tetrahedral group Td. The first-order MSO interaction contributes to c_{T1} only. The second-order MSO interaction contributes to all c_Γ's. The term in c_{A1} gives the shift common to the fine structure lines.

We will now consider the vibronic energy levels corresponding to a coupling to ε-vibrational modes. (Detailed studies of vibronic interactions and presentations of Ham's perturbation models by Ham himself can be found in Ref. 17.) When Ham's perturbation model is valid, that is, when

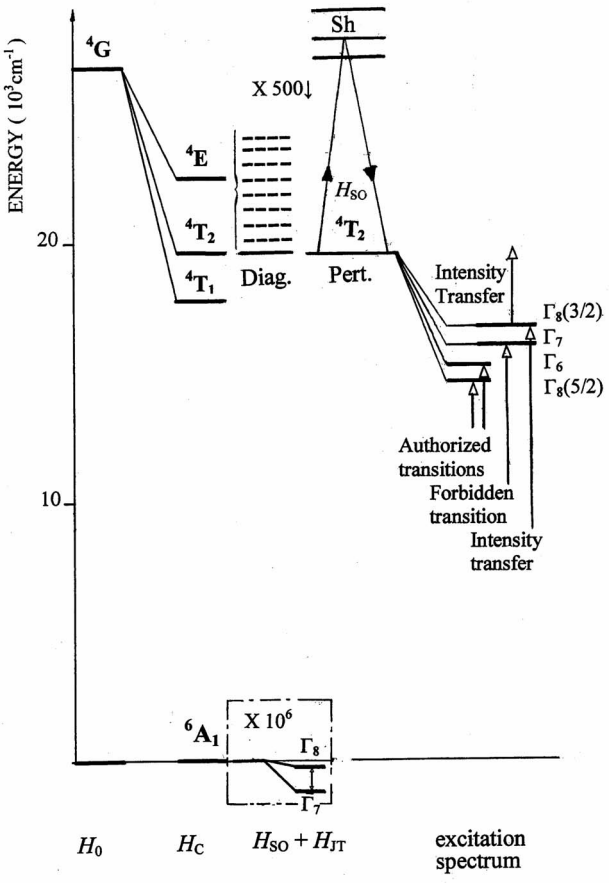

FIG. 1. Schematic representation of the adopted model. The energies of the ^4G spectroscopic term and of the $^4T_1$, $^4T_2$ and ^4E multiplets are given to the left. The diagonalization of the vibronic Hamiltonian for the $^4T_2$ level (diag.) and the second-order perturbation scheme (pert.) used to account for the influence of the excited *Sh* levels are schematically represented in the center of the figure. The fine structure of the fundamental $^6A_1$ level is represented at the bottom of the figure. The fine structure of the $^4T_2$ level is represented to the right.

the overall splitting of the electronic fine structure is smaller than both the Jahn-Teller energy E_{JT} and the energy of the effective phonon $\hbar\omega_E$, then the vibronic interactions can be described from the operator H_{eq} by replacing the c_Γ's by coefficients $c_{\Gamma JT}$ defined as follows:[17]

$$c_{T1JT} = c_{T1}e^{-3S/2} - K_1/2,$$

$$c_{EJT} = c_E + K_1 + K_2,$$

$$c_{T2JT} = c_{T2}e^{-3S/2} + K_1,$$

where $K_1 = -c_{T1}^2 f_a/\hbar\omega$ and $K_1 + K_2 = -c_{T1}^2 f_b/\hbar\omega$, with $f_a = e^{-x}G(x/2)$, $x = 3E_{JT}/\hbar\omega$, $G(x) = \Sigma x^n/n(n!)$, $f_b = e^{-x}G(x)$. E_{JT} is the Jahn-Teller energy and $\hbar\omega$ is the energy of an effective phonon of E symmetry. The Huang-Rhys S factor is defined as $S = E_{JT}/\hbar\omega$.

B. Diagonalization of the vibronic Hamiltonian for a $^4T_2$ multiplet and perturbation scheme for the vibronic coupling with the other multiplets of the d^5 configuration

As shown in Ref. 4, the vibronic model presented in Sec. II A cannot account for the amplitude of the fine structure lines of the $^4T_2$ level of Mn^{2+} in ZnS and ZnSe. Therefore, a direct diagonalization of the vibronic Hamiltonian for a $^4T_2$ level and its vibrational modes has been performed (see Fig. 1).

Following Ham,[17] for a coupling to an ε-vibrational mode, the vibronic Hamiltonian H_{vib} is the sum of the electronic Hamiltonian H_e (which will include the MSO interaction), the nuclear Hamiltonian $H_n = (1/2)\mu\omega(Q_\theta^2 + Q_\varepsilon^2)I + [1/(2\mu)](P_\theta^2 + P_\varepsilon^2)I$, and the Jahn-Teller Hamiltonian $H_{JT} = V(Q_\theta E_\theta + Q_\varepsilon E_\varepsilon)$. Q_θ and Q_ε are vibrational modes of E symmetry, the Ps are the momentum conjugates to the Qs, μ and ω are the effective mass and angular frequency of an effective phonon, respectively. I is the unit matrix. E_θ and E_ε are orbital operators spanning the E representation. The coefficient V which gives the strength of the electron-nuclear coupling is related to the Jahn-Teller energy by $E_{JT} = V^2/2\mu\omega^2$.

The matrix elements of the vibronic Hamiltonian have been calculated on the basis $\{|\varphi_i, n_\theta, n_\varepsilon\rangle\}$ $(i = 1, \ldots, N;\ n_\theta = 0, \ldots, n;$ and $n_\varepsilon = n - n_\theta)$, where n is the number of phonons, n_θ and n_ε are the numbers of phonons of normal coordinates Q_θ and Q_ε, respectively, and N is the dimension of the electronic matrix whose matrix elements are denoted φ_i. For n phonons, the dimension of the vibronic basis is $N(n+1)(n+2)/2$.

By using this basis and expressing the electronic matrix elements φ_i in the spinor group T_d^*, the matrix elements of H_{vib} are

$$\begin{aligned}
&\langle ShJt\tau, n_\theta, n_\varepsilon | H_e + H_n + H_{JT} | ShJ't'\tau', n'_\theta n'_\varepsilon \rangle \\
&\quad = \delta(n_\theta, n'_\theta)\,\delta(n_\varepsilon, n'_\varepsilon)\langle ShJt\tau | H_e | ShJ't'\tau' \rangle \\
&\qquad + \delta(n_\theta, n'_\theta)\,\delta(n_\varepsilon, n'_\varepsilon)(n_\theta + n_\varepsilon + 1)\hbar\omega \\
&\qquad + (S)^{1/2}\{\delta(n_\varepsilon, n'_\theta)[\delta(n_\theta + 1, n'_\theta)(n_\theta + 1)^{1/2} \\
&\qquad + \delta(n_\theta - 1, n'_\theta)(n_\theta)^{1/2}]\langle ShJt\tau | E_\theta | ShJ't'\tau' \rangle + \delta(n_\theta, n'_\theta) \\
&\qquad \times [\delta(n_\varepsilon + 1, n'_\varepsilon)(n_\varepsilon + 1)^{1/2} + \delta(n_\varepsilon - 1, n'_\varepsilon)(n_\varepsilon)^{1/2}] \\
&\qquad \times \langle ShJt\tau | E_\varepsilon | ShJ't'\tau' \rangle\}.
\end{aligned}$$

The first and second terms to the right give the matrix elements of the electronic and nuclear Hamiltonians H_e and H_n, respectively. The third term gives the matrix elements of the Jahn-Teller Hamiltonian. Griffiths's notation *Sh* for the multiplets and $|ShJt\tau\rangle$ for the fine structure basis vectors in the spinor group T_d^* has been used.[21]

The first-order MSO interaction has been considered for the diagonalization. Three to ten phonons have been considered in order to check the convergency of the energies and wave functions of the fundamental vibronic levels.

The results of the diagonalization are represented in Figs. 2(a) and 2(b) for the fundamental fine structure lines of a $^4T_2(G)$ level. This figure shows the splittings and RDSs in terms of the Huang-Rhys factor $S = E_{JT}/\hbar\omega_E$ and in terms of

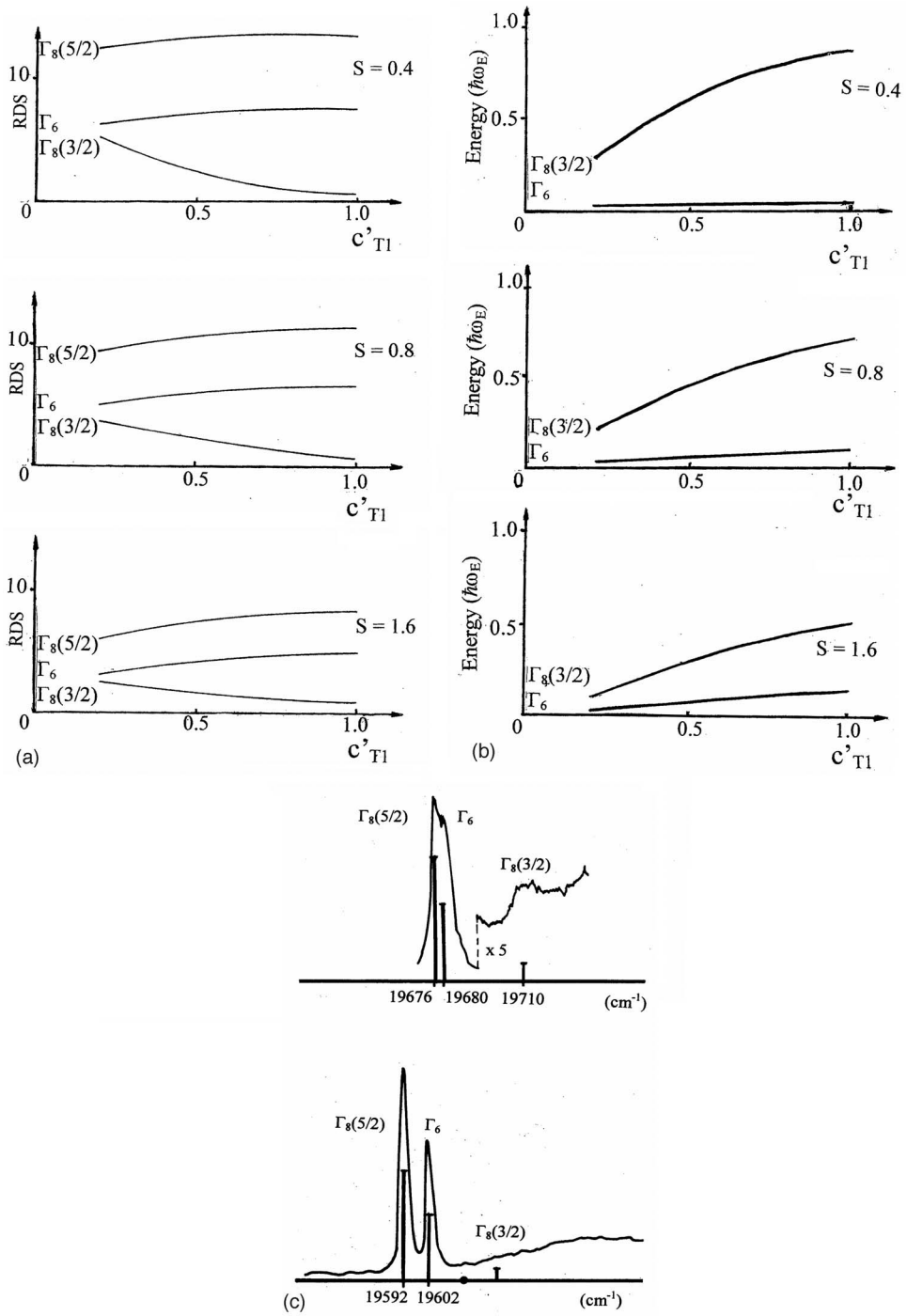

FIG. 2. (a) Relative dipole strengths (RDS's) of the fine structure lines of level ${}^4T_2(G)$ of Mn in terms of the parameter $c'_{T1}=c_{T1}$ (first order)$/\hbar\omega_E$. This figure shows the strong decrease of the amplitude of the ${}^6A_1\rightarrow\Gamma_8(3/2)$ transition when increasing c'_{T1}. (The amplitude of the ${}^6A_1\rightarrow\Gamma_7$ transition is zero in T_d symmetry.) (b) Energies of the fine structure lines in terms of c'_{T1} with respect to the energy of the $\Gamma_8(5/2)$ fine structure line. These energies are obtained from the diagonalization of the vibronic Hamiltonian of the ${}^4T_2(G)$ level. (c) Energy levels and relative dipole strengths for the ${}^4T_2(G)$ level of Mn in ZnS and ZnSe.

the MSO interaction expressed in units of $\hbar\omega_E$.

It is important to note that the proposed diagonalization generalizes the perturbation model proposed by Ham for the following diagonal and off-diagonal matrix elements (on a real basis T_{2x}, T_{2y}, and T_{2z}) of H_{SO}:

$$\langle {}^4T_{2i}00|H_{SO}^2|{}^4T_{2i}00\rangle = -f_b/\hbar\omega_E \sum_{j\neq i}\langle {}^4T_{2i}|H_{SO}|{}^4T_{2j}\rangle \times\langle {}^4T_{2j}|H_{SO}|{}^4T_{2i}\rangle$$

and

$$\langle {}^4T_{2i}00|H_{SO}^2|{}^4T_{2j}00\rangle = -f_a/\hbar\omega_E \sum_{j\neq i}\langle {}^4T_{2i}|H_{SO}|{}^4T_{2k}\rangle \times\langle {}^4T_{2k}|H_{SO}|{}^4T_{2j}\rangle,$$

where i, j, or $k=x,y$, or z. In Sec. IV, we will use the fact that these matrix elements are described by the terms involving f_a and f_b in order to get the contribution of the second-order MSO interaction and of the vibronic coupling with the other multiplets *Sh* of the d^5 configuration from the perturbation model given in Sec. II A.

However, this diagonalization does not account for the influence of the other multiplets *Sh* of the d^5 configuration.

TABLE I. Contributions to the c_Γ's of the first-order and second-order MSO interaction for the $^4T_2(G)$ level of Mn in ZnS and ZnSe for the CF model (a) and for the molecular cluster model (b, c). For ZnS and ZnSe, the results are given for three sets of values for B, C, Dq. $\Delta = W\Gamma_6 - W\Gamma_8(5/2)$ as given by the electronic model (CF or molecular model). $c'_{T1} = c_{T1}$ (first order)/$\hbar\omega_E$. Except for c'_{T1} all values are in cm^{-1}. (a) CF model ($\zeta t_2 t_2 = \zeta e t_2 = 300$ cm^{-1}, $\hbar\omega_E = 70$ cm^{-1} for ZnS:Mn and 60 cm^{-1} for ZnSe:Mn). (b) ZnS:Mn. Covalent model ($\zeta t_2 t_2 = 178$ cm^{-1}, $\zeta e t_2 = 236$ cm^{-1}; $\hbar\omega_E = 70$ cm^{-1}). (c) ZnSe:Mn. Covalent model ($\zeta t_2 t_2 = -139$ cm^{-1}, $\zeta e t_2 = 194$ cm^{-1}; $\hbar\omega_E = 60$ cm^{-1}).

	B	C	Dq	c_{A1}	c_E	c_{T2}	c_{T1} First order	c_{T1} Second order	c'_{T1} ZnS	c'_{T1} ZnSe	Δ
						(a)					
ZnS, ZnSe	630	3040	−540	−8.76	3.09	0.06	−33.98	3.93	−0.49	−0.57	−5.40
ZnS	730	2880	−420	−8.61	1.57	−1.16	−31.58	3.53	−0.45		−4.86
ZnSe	740	2740	−405	−8.98	1.45	−1.29	−31.20	3.74		−0.52	−4.91
ZnS, ZnSe	830	2500	−450	−9.89	1.56	−1.05	−32.75	4.71	−0.47	−0.55	−4.67
						(b)					
ZnS	630	3040	−540	−5.25	1.65	0.57	−30.86	2.11	−0.44		−1.93
Covalent	730	2880	−420	−5.11	0.72	−0.25	−27.57	1.96	−0.39		−1.75
model	830	2500	−450	−5.80	0.75	−0.16	−28.59	2.64	−0.41		−1.64
						(c)					
ZnSe	630	3040	−540	−3.42	0.35	1.74	−46.16	0.50		−0.77	2.51
Covalent	740	2740	−405	−3.48	−0.56	1.22	−35.64	0.49		−0.59	3.22
model	830	2500	−450	−3.86	−0.38	1.44	−37.68	0.70		−0.63	3.32

Following Sturge, the contribution of the other multiplets is given by the matrix elements (see Fig. 1)[22]

$$\langle {}^4T_{2i}00|H_{SO}^2|{}^4T_{2i}00\rangle = \sum_{Sh} \langle {}^4T_{2i}|H_{SO}|Sh\rangle \times \langle Sh|H_{SO}|{}^4T_{2i}\rangle / [W({}^4T_2) - W(Sh)]$$

and

$$\langle {}^4T_{2i}00|H_{SO}^2|{}^4T_{2j}00\rangle = e^{-3S/2} \sum_{Sh} \langle {}^4T_{2i}|H_{SO}|Sh\rangle \times \langle Sh|H_{SO}|{}^4T_{2j}\rangle / [W({}^4T_2) - W(Sh)]$$

The nonreduced diagonal term is described by c_E, and the reduced off-diagonal term is described by the terms $c_{T1}e^{-3S/2}$ and $c_{T2}e^{-3S/2}$ defined in Sec. II A. These relations are valid if $|W({}^4T_2) - W(Sh)| \gg \hbar\omega_E$. It can be noted here that this condition is satisfied for the considered $^4T_2(G)$ levels of Mn in ZnS and ZnSe, so that it is not necessary to consider higher-order perturbation schemes for vibronic interactions.

In Sec. IV, the splittings of the vibronic lines will be obtained by adding the splittings given by the diagonalization of the vibronic Hamiltonian for the $^4T_2$ level to the splittings given by the contribution of the other multiplets of the d^5 configuration.

III. ELECTRONIC AND VIBRONIC STRUCTURES FOR THE $^4T_2(G)$ LEVEL OF Mn^{2+} IN ZnS AND ZnSe FROM HAM'S PERTURBATION MODEL

The monoelectronic wave functions in Td symmetry have been determined from a self-consistent linear combination of atomic orbitals-molecular orbitals (LCAO-MO) method described *in extenso* in Ref. 22. Four sets were obtained by slightly varying the interatomic distance to account for the covalent radius of the cation. These sets correctly account for the cubic crystal-field parameter Dq, for the orbit-lattice coupling coefficients (OLCCs) to E strains of the $^4T_1(G)$ levels,[23] and for the spin-lattice coupling coefficients (SLCCs) of the $^6A_1$ fundamental level of Mn in ZnS and ZnSe.[24] These sets have recently been used to interpret the fine structure of the $^4T_1(G)$ levels.[1] Among the four sets, two sets also correctly account for the lifetimes of the fluorescent level of Mn in ZnS and ZnSe.[25] These two sets are used in the following to interpret the molecular electronic structures of $^4T_2(G)$ levels.

The multielectronic wave functions are calculated from the values of B, C, and Dq which correctly accounted for the experimental energy levels $^4T_1(G)$, $^4T_2(G)$, and $^4E(G)$. Several sets for B, C, and Dq have been considered in order to determine their influence on the splittings of the studied $^4T_2(G)$ level.

For ZnS:Mn, the first set of monoelectronic wave functions corresponds to an interatomic distance of $a = 4.41$ a.u., the crystal electric field is $C_{mad} = 1.63$. In the molecular model, C_{mad} is defined as follows: for the cation and the ligands, the crystal electric field of the four nearest neighbors and of the 12 next-nearest neighbors has been calculated directly. The contribution of the other ions to the crystal electric field is given by their contribution, denoted C_{mad}, to the Madelung energy. The charge of the lattice is $Q_{lat} = \pm 0.8$, the charge of the cation is $Q_M = 1.31$, and the theoretical value for the cubic field coefficient is $Dq = -365$ cm^{-1}. The spin-orbit coupling constants are $\zeta_{3d} = 301$ cm^{-1} for the d electrons of Mn and $\zeta_{3p} = 302$ cm^{-1} for the p electrons of sulfur. The matrix elements of τ are $\zeta e t_2 = 236$ cm^{-1} and

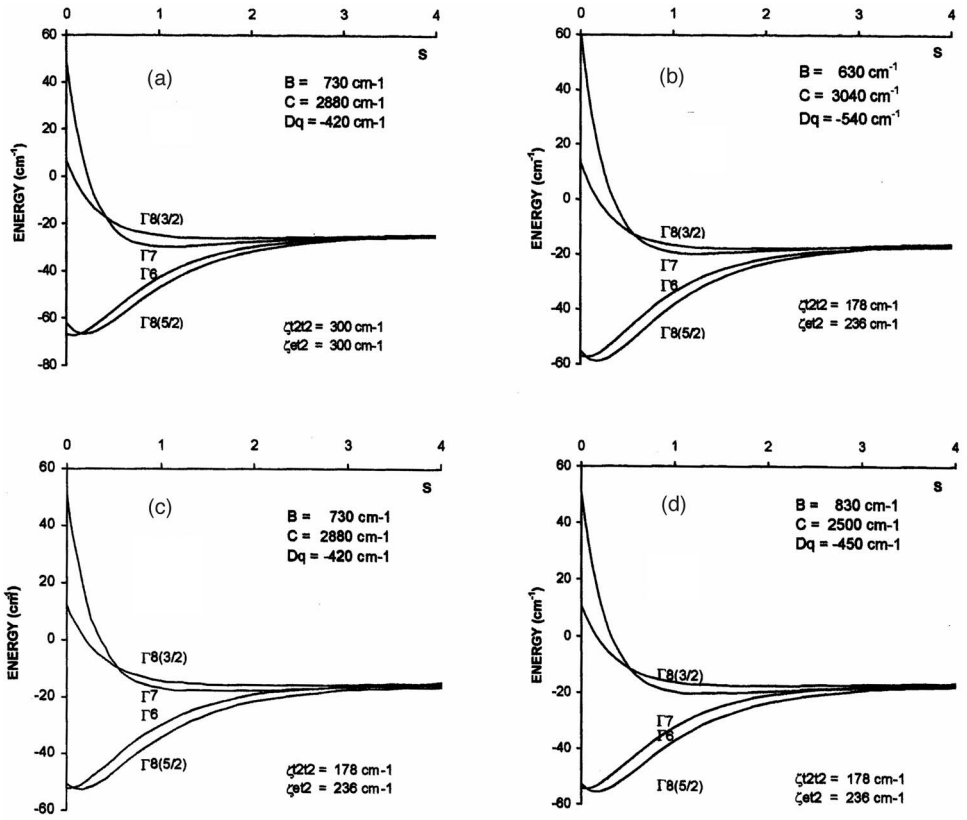

FIG. 3. Theoretical splitting of the ${}^4T_2(G)$ level of Mn in ZnS in terms of the Huang-Rhys factor S as predicted by Ham's perturbation model. (a) gives the energy levels as predicted by the CF model. (b), (c), and (d) correspond to the molecular model for three sets of values for B, C, and Dq and for $\zeta t_2 t_2 = 178\ \mathrm{cm}^{-1}$ and $\zeta et_2 = 236\ \mathrm{cm}^{-1}$. $\hbar\omega_E = 70\ \mathrm{cm}^{-1}$.

$\zeta t_2 t_2 = 178\ \mathrm{cm}^{-1}$. The second set of monoelectronic wave functions corresponds to $a = 4.56$ a.u., $C_{mad} = 1.40$, $Q_{lat} = \pm 0.8$, $Q_M = 0.97$, $Dq = -419\ \mathrm{cm}^{-1}$, $\zeta_{3d} = 285\ \mathrm{cm}^{-1}$, $\zeta_{3p} = 308\ \mathrm{cm}^{-1}$, $\zeta et_2 = 205\ \mathrm{cm}^{-1}$, and $\zeta t_2 t_2 = 131\ \mathrm{cm}^{-1}$.

The multielectronic wave functions are obtained from three sets of values for B, C, and Dq, which correctly account for the experimental energy levels of Mn in ZnS (see Table I).

The vibronic structures of levels ${}^4T_2(G)$ of Mn in ZnS are represented in Fig. 3 in terms of the Huang-Rhys factor S, in the case of a coupling to ε-vibrational modes. Since, for the CF model, the energy level scheme does not significantly depend on the values for B, C, and Dq, only one scheme corresponding to $B = 730\ \mathrm{cm}^{-1}$, $C = 2880\ \mathrm{cm}^{-1}$, and $Dq = -420\ \mathrm{cm}^{-1}$ is represented [see Fig. 3(a)]. The vibronic molecular structures are given in Figs. 3(b)–3(d), for $\zeta et_2 = 236\ \mathrm{cm}^{-1}$, $\zeta t_2 t_2 = 178\ \mathrm{cm}^{-1}$, and for the three chosen sets of values for B, C, and Dq. The energy level schemes for $\zeta et_2 = 205\ \mathrm{cm}^{-1}$ and $\zeta t_2 t_2 = 131\ \mathrm{cm}^{-1}$, which are almost identical to those given in Fig. 3, are not represented.

Figure 3 clearly shows that for ZnS:Mn the energy level schemes as given by the CF and molecular models are almost identical.

For ZnSe: Mn, the first set of monoelectronic wave functions corresponds to $a = 4.61$ a.u., $C_{mad} = 1.63$, $Q_{lat} = \pm 0.7$, $Q_M = 1.22$, $Dq = -310\ \mathrm{cm}^{-1}$, $\zeta_{3d} = 296\ \mathrm{cm}^{-1}$ for Mn, $\zeta_{4p} = 1404\ \mathrm{cm}^{-1}$ for selenium, $\zeta et_2 = 194\ \mathrm{cm}^{-1}$, and $\zeta t_2 t_2 = -139\ \mathrm{cm}^{-1}$. The second set corresponds to $a = 4.76$ a.u., $C_{mad} = 1.33$, $Q_{lat} = \pm 0.7$, $Q_M = 0.84$, $Dq = -421\ \mathrm{cm}^{-1}$, $\zeta_{3d} = 274\ \mathrm{cm}^{-1}$, $\zeta_{4p} = 1442\ \mathrm{cm}^{-1}$, $\zeta et_2 = 150\ \mathrm{cm}^{-1}$, and $\zeta t_2 t_2 = -270\ \mathrm{cm}^{-1}$.

Three sets of values for B, C, and Dq are considered (see Table I). Since the experimental energy levels are almost identical in ZnS and ZnSe, two sets for B, C, and Dq are chosen to be identical.

The theoretical vibronic structures of level ${}^4T_2(G)$ of Mn in ZnSe are given in Fig. 4. The energy levels as given by the CF model are given in Figs. 4(a) and 4(b) for $B = 630\ \mathrm{cm}^{-1}$, $C = 3040\ \mathrm{cm}^{-1}$, $Dq = -540\ \mathrm{cm}^{-1}$, and for $B = 740\ \mathrm{cm}^{-1}$, $C = 2740\ \mathrm{cm}^{-1}$, $Dq = -405\ \mathrm{cm}^{-1}$. For $B = 830\ \mathrm{cm}^{-1}$, $C = 2500\ \mathrm{cm}^{-1}$, and $Dq = -450\ \mathrm{cm}^{-1}$, the energy levels are almost identical to those obtained by taking $B = 740\ \mathrm{cm}^{-1}$, $C = 2740\ \mathrm{cm}^{-1}$, and $Dq = -405\ \mathrm{cm}^{-1}$. The energy levels, as given by the molecular model, are shown in Figs. 4(c) and 4(d), for the preceding values for B, C, Dq, and for $\zeta et_2 = 194\ \mathrm{cm}^{-1}$, $\zeta t_2 t_2 = -139\ \mathrm{cm}^{-1}$. For $\zeta et_2 = 150\ \mathrm{cm}^{-1}$ and $\zeta t_2 t_2 = -270\ \mathrm{cm}^{-1}$, the energy levels are almost identical to those obtained by taking $\zeta et_2 = 194\ \mathrm{cm}^{-1}$, $\zeta t_2 t_2 = -139\ \mathrm{cm}^{-1}$.

Figure 4 shows that, for $S = 0$, the overall splitting of the fine structure lines is of 110–120 cm^{-1} for the CF model and of 150–200 cm^{-1} for the molecular model. Furthermore, for $0.2 < S < 2$, the splitting of the two levels $\Gamma_8(5/2)$ and Γ_6 at lower energy, is larger in the molecular model than in the CF model. *The strong increase of the first- and second-order MSO splittings is primarily due to the fact that the spin-orbit coupling constant of the p electrons of selenium is approximately four times greater than that of sulfur.*

IV. COMPARISON WITH EXPERIMENTS

For the ${}^4T_2(G)$ level of Mn^{2+} in ZnS, excitation experiments, uniaxial stress experiments,[4] and magnetic field

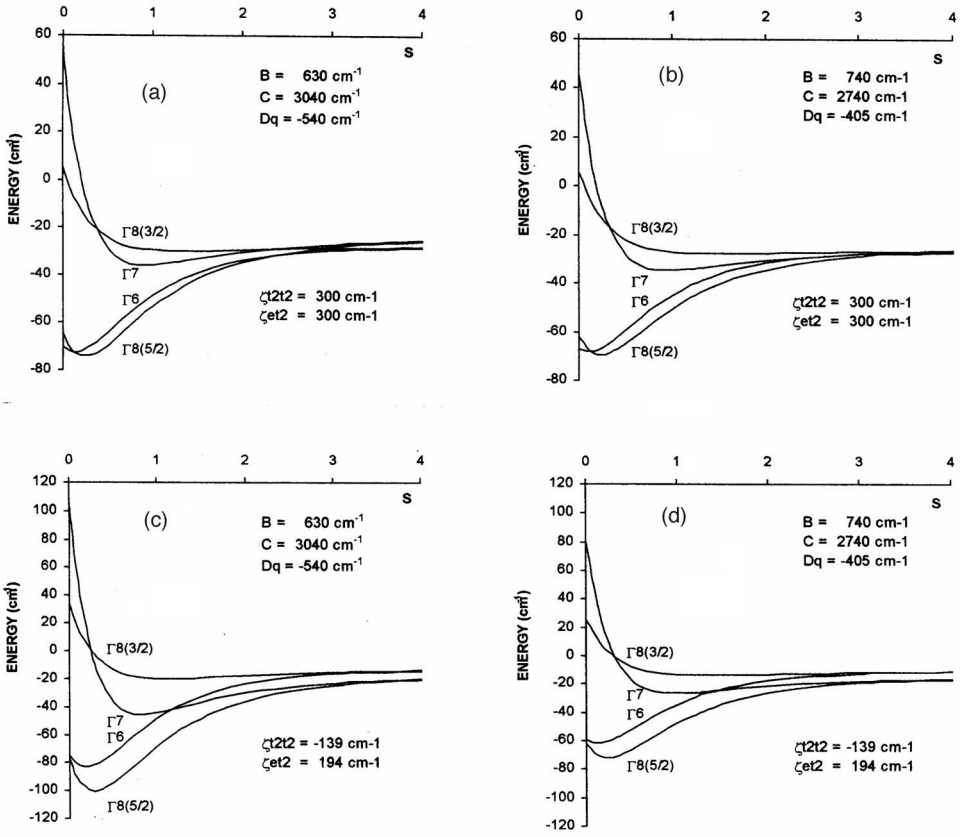

FIG. 4. Theoretical splitting of level $^4T_2(G)$ of Mn in ZnSe in terms of the Huang-Rhys factor S. (a) gives the energy levels as predicted by the CF model. (b), (c), and (d) correspond to the molecular model for three sets of values for B, C, Dq and for $\zeta t_2 t_2 = -139$ cm^{-1} and $\zeta et_2 = 194$ cm^{-1}. $\hbar\omega_E = 60$ cm^{-1}.

experiments[5] performed at $T=2.2$ K on pure cubic crystals, that is, without stacking faults, have shown that the three excitation lines are associated with levels $\Gamma_8(5/2)$ at 19 676 cm^{-1}, Γ_6 at 19 680 cm^{-1}, and $\Gamma_8(3/2)$ at 19 710 cm^{-1} [see Fig. 2(c)], and that the coupling is to E strains only. Therefore, with respect to the energy of the $\Gamma_8(5/2)$ level, the energies are $W\Gamma_6=4$ cm^{-1} and $W\Gamma_8(3/2)=34$ cm^{-1}.

Figure 3 shows that the energies of the observed fine structure lines can be correctly accounted for, either by the CF model or by the molecular model, by taking $S=0.5-1$ and $\hbar\omega=70$ cm^{-1}. However, following these models, the predicted RDS's are 14, 7, 0, and 9 for the transitions to levels $\Gamma_8(5/2)$, Γ_6, Γ_7, and $\Gamma_8(3/2)$, respectively, so that these models cannot account for the relative dipole strength of the weak line $\Gamma_8(3/2)$.

In the chosen model presented in Sec. II B the energy levels have been obtained by adding the energies obtained from the diagonalization of the vibronic Hamiltonian for the $^4T_2(G)$ level to the contribution of the other excited levels as given by the perturbation scheme presented in Section II B. The diagonalization of the vibronic Hamiltonian has been performed from the electronic states as given by the first-order MSO interaction. The molecular model gives $c'_{T1} = c_{T1}(\text{first order})/(\hbar\omega_E) = -0.44$, -0.39, and -0.41 for three sets for B, C, and Dq [see Table I(b)]. The energy of the effective phonon is $\hbar\omega=70$ cm^{-1}. For these values for c'_{T1}, the splitting $[W\Gamma_6 - W\Gamma_8(5/2)]_{diag}$ of the two observed levels is of 2.9–3.0 cm^{-1} for $S=0.4$ and of 3.9 cm^{-1} for $S=0.8$ [see Fig. 4(b)]. The energy of the $\Gamma_8(3/2)$ level is predicted to be of 33–35 cm^{-1} for $S=0.4$ and of 24.9–26.4 cm^{-1} for $S=0.8$.

We will now take into account the influence of the other excited levels of the d^5 configuration. For $S=0$, the theoretical second-order MSO splitting $\Delta=[W\Gamma_6 - W\Gamma_8(5/2)]_{el}$ is of -1.93 cm^{-1}, -1.75 cm^{-1}, and -1.64 cm^{-1} as given in Table I(b) for the three sets a, b, and c for B, C, and Dq, respectively. The contribution of the other excited levels of the d^5 configuration has been obtained by the diagonalization of the first- and second-order MSO interaction by taking $f_a=f_b=0$ in order to cancel the contribution of the MSO interaction in the $^4T_2(G)$ level. For $\Delta=-1.75$ cm^{-1}, we obtained $W\Gamma_6 - W\Gamma_8(5/2) = -1.5$ cm^{-1} for $S=0.4$ and $W\Gamma_6 - W\Gamma_8(5/2) = -1.4$ cm^{-1} for $S=0.8$. Therefore, the total splitting $W\Gamma_6 - W\Gamma_8(5/2)$ is of 1.4–1.5 cm^{-1} for $S=0.4$ and 2.5 cm^{-1} for $S=0.8$. For $S=0.8$, the total splitting of 2.5 cm^{-1} is in good agreement with the experimental value of 4 cm^{-1}.

Concerning the intensity transfer, the RDSs for the transitions $^6A_1 \rightarrow \Gamma_8(5/2)$, Γ_6, Γ_7, and $\Gamma_8(3/2)$, are 14, 7.4, 0, and 3.2–3.5 for $S=0.4$, and 14, 7.9, 0, and 3.6 for $S=0.8$, respectively. (The amplitude of the transition $^6A_1 \rightarrow \Gamma_8(5/2)$ is taken to be 14 in order to easily compare the RDSs given by the considered models.)

For the $^4T_2(G)$ level of Mn^{2+} in ZnSe, excitation experiments, uniaxial stress experiments,[4] and magnetic field experiments[5] performed at $T=2.2$ K have shown that the two observed excitation lines are to be associated with levels $\Gamma_8(5/2)$ at 19 592 cm^{-1} and Γ_6 at 19 602 cm^{-1}, the coupling being to E strains only [see Fig. 2(c)].

The diagonalization of the vibronic Hamiltonian has been performed from the electronic states as given by the first-

order MSO interaction. The molecular model gives $c'_{T1}=c_{T1}$ (first order)$/(\hbar\omega_E)=-0.77$, -0.59, and -0.63 for three sets for B, C, and Dq [see Table I(c)]. The energy of the effective phonon is $\hbar\omega=60$ cm^{-1}. For these values for c'_{T1}, the splitting $[W\Gamma_6-W\Gamma_8(5/2)]_{diag}$ of the two observed levels is of 2.6–2.7 cm^{-1} for $S=0.4$ and of 4–5 cm^{-1} for $S=0.8$ [see Fig. 2(b)]. The energy of the $\Gamma_8(3/2)$ level is predicted to be of 40–47 cm^{-1} for $S=0.4$ and of 29–36 cm^{-1} for $S=0.8$.

We will now consider the influence of the other excited levels of the d^5 configuration. For $S=0$, the theoretical second-order MSO splitting $\Delta=[W\Gamma_6-W\Gamma_8(5/2)]_{el}$ is +2.51 cm^{-1}, +3.22 cm^{-1}, and +3.32 cm^{-1} as given in Table I(c) for three sets for B, C, and Dq, respectively. For $\Delta=+3.22$ cm^{-1}, we obtained $W\Gamma_6-W\Gamma_8(5/2)=2.8$ cm^{-1} for $S=0.4$ and 2.6 cm^{-1} for $S=0.8$.

The total splitting $W\Gamma_6-W\Gamma_8(5/2)$ is of 5.4–5.5 cm^{-1} for $S=0.4$ and of 6.6–7.6 cm^{-1} for $S=0.8$. These splittings are in good agreement with the experimental value of 10 cm^{-1}.

Concerning the intensity transfer, the RDSs of the transitions ${}^6A_1\rightarrow\Gamma_8(5/2)$, Γ_6, Γ_7, and $\Gamma_8(3/2)$ are 14, 8, 0, and 1.5 for $S=0.4$ and 14, 7.9, 0, and 1.8 for $S=0.8$.

V. CONCLUSION

Molecular and vibronic cluster models have been used to account for the molecular electronic structure and the vibronic coupling to ε-vibrational modes of the ${}^4T_2$ levels of d^5 ions in tetrahedral symmetry.

First, a molecular cluster model involving the four nearest neighbors of the cation and the nearest neighbors of the ligands has been used to determine the monoelectronic wave functions. The influence of the remaining ions of the crystal has been represented by their contribution to the Madelung energy. The multielectronic wave functions for all levels associated with the d^5 configuration have been determined from the diagonalization of the matrices of Sugano *et al.* Finally, the molecular electronic structure has been determined from the first- and second-order MSO interaction and the results have been compared to those given by the well-known CF model. When comparing the theoretical electronic structures of the ${}^4T_2$ level in ZnS and ZnSe, it has been shown that the first-order MSO interaction in ZnS is almost identical to the electronic structure predicted by the CF model while there is a strong increase of the first- and second-order MSO interaction in ZnSe. This is due to the fact that the spin-orbit coupling constants ζ_L of the p electrons of Se are approximatively four times greater than the spin-orbit coupling constants ζ_M of the d electrons of Mn^{2+}, while for ZnS, ζ_L is almost identical to ζ_M.

Second, Ham's cluster and perturbation models have been considered to analyze the vibronic coupling to ε-vibrational modes and the energies of the vibronic levels of the ${}^4T_2$ levels. However, the perturbation model did not correctly account for the RDSs of the fine structure lines.

Third, in order to explain the selective intensity transfer observed in the case of Mn^{2+} in ZnS and ZnSe, the vibronic Hamiltonian for the ${}^4T_2$ level has been diagonalized and the vibronic interactions with all other multiplets have been calculated. It has been shown that this model very well accounts for the energies and RDSs of the fine structure lines. More generally, it has been shown that, when the energy $\hbar\omega_E$ of the effective phonon is (i) less than the overall splitting of the electronic levels due to the spin-orbit interaction; and (ii) not very different from the Jahn-Teller energy E_{JT}, then, the energy levels of the fine structure lines and the intensity transfers can be very accurately accounted for by considering the MSO interaction, the direct diagonalization of the vibronic Hamiltonian for the considered orbital triplet, and the contribution of the other multiplets of the d^5 configuration from a second-order perturbation scheme.

Finally, it can be noted that the proposed cluster models could be used, at the expense of slight modifications concerning the influence of the ions located outside the molecular cluster, to predict the fine structure of the excited levels of cubic or nearly cubic Mn^{2+} centers in NCs.

ACKNOWLEDGMENTS

Thanks are due to F. S. Ham, A. Dörnen, and C. Naud for very helpful comments and discussions on vibronic interactions.

[1] D. Boulanger and R. Parrot, Phys. Rev. B **66**, 205201 (2002).
[2] D. Boulanger, R. Parrot, M. N. Diarra, U. W. Pohl, B. Litzenburger, and H. E. Gumlich, Phys. Rev. B **58**, 12567 (1998).
[3] G. Hofmann, F. G. Anderson, and J. Weber, Phys. Rev. B **43**, 9711 (1991).
[4] R. Parrot, C. Naud, and F. Gendron, Phys. Rev. B **13**, 3748 (1976).
[5] R. Parrot and D. Boulanger, Phys. Status Solidi B **207**, 113 (1998).
[6] R. Parrot and D. Boulanger, Physica B **340-342**, 267 (2003).
[7] A. Hoffmann, R. Heitz, and I. Broser, Phys. Rev. B **41**, 5806 (1990).
[8] R. Heitz, A. Hoffmann, and I. Broser, Phys. Rev. B **45**, 8977 (1992).
[9] K. Pressel, G. Rückert, A. Dörnen, and K. Thonke, Phys. Rev. B **46**, 13171 (1992); K. Pressel, G. Bohnert, G. Rückert, A. Dörnen, and K. Thonke, J. Appl. Phys. **71**, 5703 (1992).
[10] R. Heitz, P. Thurian, I. Loa, L. Eckey, A. Hoffmann, I. Broser, K. Pressel, B. K. Meyer, and E. N. Mokhov, Appl. Phys. Lett. **67**, 2822 (1995).
[11] R. Heitz, P. Maxim, L. Eckey, P. Thurian, A. Hoffmann, I. Broser, K. Pressel, and B. K. Meyer, Phys. Rev. B **55**, 4382 (1997).
[12] K. Pressel, G. Bohnert, A. Dörnen, B. Kaufmann, J. Denzel, and K. Thonke, Phys. Rev. B **47**, 9411 (1993).
[13] R. N. Bhargava, D. Gallagher, X. Hong, and A. Nurmikko, Phys. Rev. Lett. **72**, 416 (1994).
[14] B. A. Smith, J. Z. Zhang, A. Joly, and J. Liu, Phys. Rev. B **62**, 2021 (2000).

[15] D. J. Norris, Nan Yao, F. T. Charnock, and T. A. Kennedy, Nano Lett. **1**, 1 (2001).
[16] W. Chen, R. Sammynaiken, Y. Huang, J. O. Malm, R. Wallenberg, J. O. Bovin, V. Zwiller, and N. A. Kotov, J. Appl. Phys. **89**, 1120 (2001).
[17] F. S. Ham, Phys. Rev. **138**, A1727 (1965); F. S. Ham, in *Electron Paramagnetic Resonance*, edited by S. Geschwind (Plenum, New York, 1972).
[18] A. A. Misetich and T. Buch, J. Chem. Phys. **42**, 2524 (1964).
[19] S. Sugano, Y. Tanabe, and H. Kamimura, in *Multiplets of Transition Metal Ions in Crystals* (Academic, New York, 1970).
[20] J. S. Griffith, in *The Theory of Transition-Metal Ions* (Cambridge University Press, Cambridge, 1971).
[21] J. S. Griffith, in *The Irreducible Tensor Method for Molecular Symmetry Groups* (Prentice-Hall, Englewood Cliffs, NJ, 1962).
[22] M. D. Sturge, in *Solid State Physics* (Academic, New York, 1967), Vol. 20.
[23] D. Boulanger and R. Parrot, J. Chem. Phys. **17**, 1469 (1987).
[24] R. Parrot and D. Boulanger, Phys. Rev. B **47**, 1849 (1993).
[25] D. Boulanger, R. Parrot, and Z. Cherfi, Phys. Rev. B **70**, 075209 (2004).